Convolutional Neural Network Approach for White Blood Cells Classification

Nandhini R
Department of Computer Science and Engineering

Sethu Institute of Technology
Virudhunagar, India.
nandhinirm92@gmail.com

Pabitha muthu P
Department of Computer Science and Engineering

Sethu Institute of Technology
Virudhunagar, India.
pabithapraveenit@sethu.ac.in

Abstract— White blood cells (WBCs) or leukocytes are immune cells responsible for protecting the body against infections, engulfing foreign invaders, repairing tissue injuries, and resisting pathogens or diseases. WBCs such as macrophages, neutrophils, T cells, and natural killer cells (NK cells) are essential players in many important diseases. For example, in cancer, WBCs remodel the tumor extracellular matrix, facilitate tumor cell migration and invasion, and modulate tumor angiogenesis. Through these activities, WBCs promote all stages of tumor progression. The system is developed the DL algorithms such as convolutional neural network for predicting the types of blood cell disease. Finally, the system can estimate some performance metrics such as accuracy and error rate.

Keywords—Image Segmentation, White blood cells, Convolutional Neural Network, Deep learning, Blood leukocytes segmentation.

I. INTRODUCTION

A blood cell, also called a hematopoietic cell, HEMOCYTE, or HEPATOCYTE, is a cell produced through HEMATOPOIESIS and found mainly in the blood. Major types of blood cells include red blood cells (erythrocytes), white blood cells (leukocytes), and platelets (thrombocytes). Together, these three kinds of blood cells add up to a total 44% of the blood tissue by volume, with the remaining 56% of the volume composed of plasma, the liquid component of blood.

Cell morphology is a crucial aspect of many biological processes and it has direct implications for human health. In particular, ANALYZING this characteristic of blood cells can help to provide important information that facilitates the diagnosis of some diseases or pathologies, such as DREPANOCYTE (or sickle cell) ANEMIA, HEMOLYTIC ANEMIA transmitted via autosomal recessive inheritance, and variable, habitually serious, intensity.

AUTOMATIC segmentation is a significant task in image processing applications. It has an important role in the detection, classification, and diagnosis of HEMATOLOGICAL disorders: sickle cell ANEMIA (SCA), acute lymphoblastic LEUKEMIA (ALL), and acute myeloid LEUKEMIA (AML). SCA causes significant morphological variations of red blood cells (RBCs). However, AML and ALL affect white blood cells (WBCs). Hence, the analysis of cell morphology has a vital role in the diagnosis of HAEMATOLOGICAL disorders,

Manual counting and segmentation of cells are time-consuming and truly are a more challenging job. The presence of noise, unwanted cells, overlapped cells, and poor contrast make this task more difficult. On the other hand, automatic segmentation enhances the robustness and, thus, makes diagnosis and treatment planning more accurate.

Red blood cells (RBCs) must be highly deformable to transit through the microvasculature to deliver oxygen to tissues. The loss of RBC deformability resulting from pathology, natural aging, or storage in blood bags can impede the proper function of these cells. Various methods have been developed to measure RBC deformability, but these methods require specialized equipment, long measurement time, and highly skilled personnel. To address this challenge, we investigated whether a machine-learning approach could be used to predict donor RBC deformability based on morphological features from single-cell microscope images.

We used the microfluidic ratchet device to sort RBCs based on deformability. Sorted cells are then imaged and used to train a deep-learning model to classify RBC-based image features related to cell deformability. This model correctly predicted the deformability of individual RBCs with $81 \pm 11\%$ accuracy averaged across ten donors. Using this model to score the deformability of RBC samples was accurate to within $10.4 \pm 6.8\%$ of the value obtained using the microfluidic ratchet device.

II. LITERATURE REVIEW

K. Mishra et al. proposed that a type-2 AWSFCM clustering algorithm is introduced for brain MR tissue segmentation. The proposed algorithm offers a solution to the problem of equidistant pixels, assigning them to a single cluster by providing greater weights to the pixel closer to the expected decision boundary. The spatial information of the neighboring pixels is attained using the adaptive Gaussian filter, where the order of the filter decreases with the convergence of the algorithm to the final cluster centers. A type-2 approach for the computation of the membership values and the cluster centers ensures a more accurate location of the cluster centers compared to the standard FCM clustering technique, in the presence of noise and IIH. Furthermore, the fuzzy value of the linguistic fuzzifier (M) obtained using the α-plane representation results in more accurate cluster centers.

Pradeep Kumar Das and Priyanka Jadoun presented an efficient scheme to detect healthy and unhealthy (ALL) - lymphocytes. The presented CLAHE dynamically increases the contrast level of the image and also improves the image quality successfully. Then, leukocytes are extracted using a color-based k-means clustering algorithm. The scheme employs GLCM and GLRLM to extract texture features. Moreover, it also emphasizes extracting shape and color features. Finally, SVM with RBF kernel is employed to classify WBCs into healthy and ALL affected cells.

Sukadev Meher et al. proposed that the contributions of this survey article are manifold. The principal objective of the review is to give an overview of the techniques that are available in the literature for the enhancement, segmentation, feature extraction, and classification of the image containing RBCs to detect sickle cell disease. The merits and demerits of the recent methodologies are discussed. It has an important role in the diagnosis and overall treatment planning of sickle cell disease. It may create a deeper insight into the analysis of state-of-the-art methods. Various performance measures like sensitivity, specificity, accuracy, precision, F1 score, J score, and AUC are used for the quantitative analysis of these techniques.

Sahar Zafari and Tuomas Eerola presented a method to segment multiple partially overlapping approximately elliptical shape objects in silhouette images using radial symmetry. The proposed method consists of seed point extraction using Bounded Erosion and Fast Radial Symmetry Transform, contour evidence extraction using edge-to-seed point association, and contour estimation using ellipse fitting. The experiments were carried out using one synthetically generated dataset and two datasets from real-world applications. The proposed approach for seed point extraction and the segmentation method were shown to achieve high detection and segmentation accuracies and they were found to outperform the competing methods in all datasets.

Afaf Tareef et al. proposed that despite the exciting development in the field of overlapping cell segmentation from cervical cytology images during the past five years, the focus of existing methods is mainly to achieve high performance in nuclei and cytoplasm segmentation on given datasets. In this paper, we have tried to widen our objectives to include the system's applicability, speed, and straightforward implementation. For this purpose, we design MPFW; a simple and cost-effective segmentation method that is also capable of achieving superior segmentation performance than state-of-the-art methods.

III. METHODOLOGIES

A Convolutional Neural Network (CNN) is a type of deep learning algorithm that is suited well particularly for image recognition and processing tasks. It is made up of many layers, including convolutional layers, pooling layers, and fully connected layers.

The convolutional layers are the component of a CNN, where filters are applied to the input image to extract features such as edges, shapes, and textures. The output of the convolutional layers is passed through pooling layers, which are used to sample the feature maps, reducing the spatial dimensions while retaining the most important information shown in Figure 1. The output of the pooling layers is then passed through one or more fully connected layers, which are used to make a prediction or classify the image.

CNNs contain a combination of several layers that transform an image into an output the model can understand.
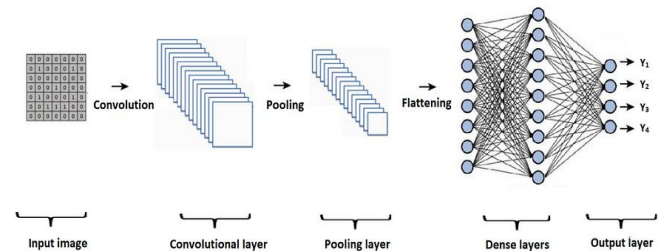

FIGURE 1. CNN Architecture

PROCESS OF CNN

Forward and backward propagation iterate through all of the training samples in the network until the optimal weights are determined and only the most powerful and predictive neurons are activated to make a prediction shown in Figure 2.
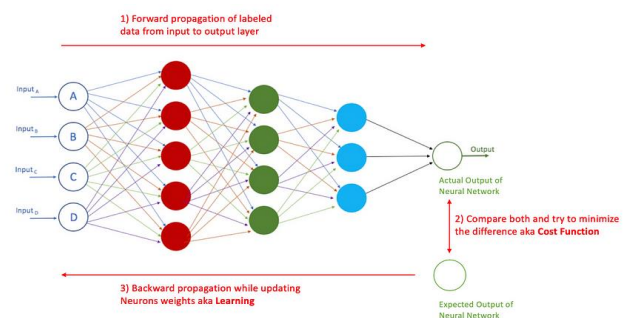

FIGURE 2: Process of CNN

The system trains throughout many epochs by taking one forward and one backward pass of all training samples each time.

Forward propagation calculates the loss and cost functions by comparing the difference between the actual and predicted target for each labeled image.

Backward propagation uses gradient descent to update the weights for each neuron, attributing more
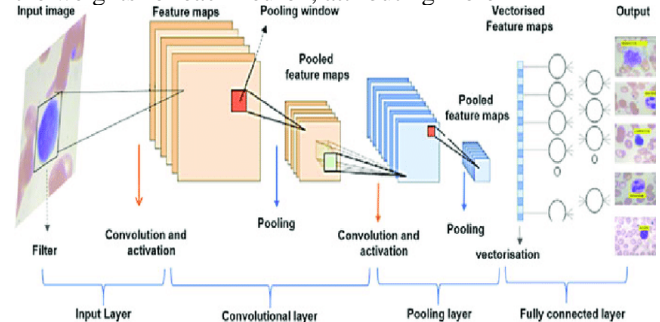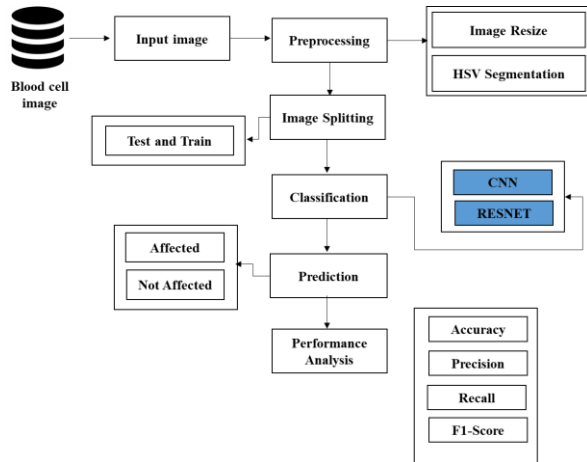

FIGURE 3: CNN Architecture for WBC Classification

B.SYSTEM ARCHITECTURE

Convolutional Neural Networks have demonstrated

remarkable

FIGURE 4: System Architecture

IV. MODULE DESCRIPTION

(a) Data selection and loading

The data selection is the process of selecting the data for the Blood cell image dataset. In this project, blood cell color images and ground truth images are used to segment the blood cell images. The dataset which contains information about the blood cell-colored images and ground truth images.

(b) Data preprocessing:

Image Data pre-processing is the process of getting rescaled data from the dataset. Resize image dataset And Get data Resize image dataset: Rescale the dataset image size into 256*256. Getting data: Categorical data is defined as variables with a finite set of rescaled values. Most deep learning algorithms require array input and output variables.

(c) Splitting dataset into train and test data:

Data splitting is the act of partitioning available data into two portions, usually for cross-validate purposes shown in Figure 4. One Portion of the data is used to develop a predictive model and the other to evaluate the model's performance. Separating image data into training and testing sets is an important part of evaluating image processing models. Typically, when you separate data into a training set and testing set, most of the image data is used for training, and a smaller portion of the data is used for testing.

(d) Classification:

A CNN is a kind of network architecture for deep learning algorithms and is specifically used for image recognition and tasks that involve the processing of data. There are some other types of neural networks in deep learning, for identifying and recognizing objects, CNNs are the network architecture of choice. A Residual Neural Network (a.k.a. Residual Network, ResNet) is a deep learning model in which the weight layers learn residual functions concerning the layer inputs. A Residual Network is a network with skip connections that perform identity mappings, merged with the layer outputs by addition.

(e) Result generation:

The Final Result will get generated based on the overall classification and prediction. The performance of this proposed approach is evaluated using some measures like,

• Accuracy

• Error rate.

V. EXPERIMENTAL ANALYSIS

In this study, the experimental software and hardware configuration are shown in Table 1.

TABLE 1. Software and hardware configuration.

Name	Model and Parameters
CPU	Intel Core i7-14700K
OS	Windows 11
GPU	GTX 1080Ti
Development Language	Python
Environment	SPYDER

A. Dataset And Preprocessing

The blood image data used in this study were obtained from the public blood cell dataset, which contained 100 images with a resolution of 300 300 pixels (Gravity Open Datasets/WBC Image Dataset 2 Gravity). Manual annotation was performed using LabelMe software.

The dataset was expanded to 500 blood cell images using augmentation processes such as rotation, zooming, and random cropping to enhance the data sample. Eighty percent of the entire dataset was used as the training set, and 20% was used as the test set.

B. Segmentation Evaluation Criteria

To quantitatively evaluate the segmentation results of the algorithm, the following evaluation indicators were mainly used: intersection over union (IOU), recall, and accuracy (ACC), The formula is shown in Equations B.

$$IOU = \frac{TP}{TP + FP + FN}$$

$$Recall = \frac{TP}{TP + FN}$$

$$ACC = \frac{TP + TN}{TP + TN + FP + FN}$$

where TP is the correct number of pixels for white blood cell segmentation in pixel-level segmentation, that is the pixel point that is predicted to be a white blood cell and is correctly predicted. TN is the number of pixels for background segmentation in pixel-level segmentation, that is, the pixel points that are predicted to be background and are correctly predicted. FN is the number of pixels for background segmentation in pixel-level segmentation, that is, the pixel

points that are predicted to be background but are predicted wrong. FP is the number of pixel points with incorrect leukocyte segmentation in pixel-level segmentation, that is, pixels predicted to be leukocytes but predicted incorrectly.

C. Comparative Experiment

To verify the segmentation performance of the improved model, two mainstream medical image segmentation models were selected for comparison: ResUNet and DeepLabv3. At the same time, it is compared with the model MIF-Net proposed in 2022 for blood cell segmentation. The segmentation results of the different models are shown in Figure 8, where

- (a) is the image information of blood cells,
- (b) is the labels of manually segmented blood leukocytes,
- (c) is the segmentation result of the original U-Net model,
- (d) is the segmentation result of the ResUNet model, (e)is the segmentation result of the DeepLabv3 model,
- (e) is the segmentation result of the MIF-Net model, and
- (f) is the segmentation result of the model in this study. The quantitative evaluation indicators for the segmentation results are presented in Table 5.

| Model	IOU (%)	Recall (%)	Acc (%)
U-Net[17]	91.1	91.7	97.9
ResUNet[32]	92.0	92.5	98.1
DeepLabV3+[14]	93.9	94.5	98.5
MIF-Net[33]	95.3	96.2	98.4
CBAM-DC-UNet	96.2	97.4	99.1

It can be seen from the figure 8 that the model in this study can segment the morphology of the leukocytes more accurately. Compared to the comparison model, the boundary segmentation is clearer, which can reduce the influence of the adhesion of surrounding erythrocytes. It can be seen from the quantitative evaluation indicators that the CBAM-DC-UNet model in this study showed better results for all indicators. As shown in Table 5, CBAM-DC-UNet can achieve 96.2% and 99.1% in IOU and Acc evaluation indicators, respectively, which are 4.2% and 1% higher than the results of the ResUNet network, respectively. Compared with DeepLabv3, these two indicators are 2.3% and 0.6%, respectively. Compared to MIF-Net, these two indicators improved by 0.9% and 0.7%, respectively. It can be seen that the network in this paper has better performance in the segmentation of blood leukocytes.

Original Image
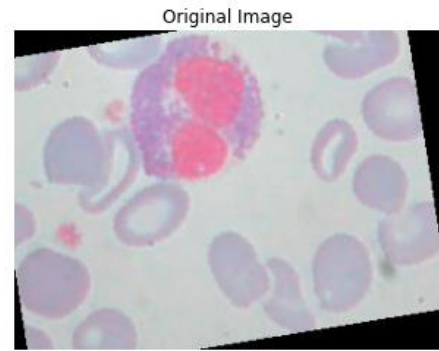
RESIZED IMAGE
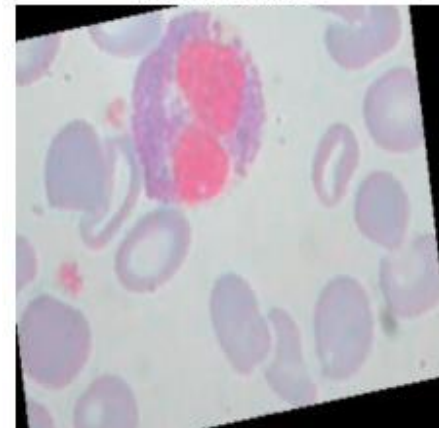
GRAY SCALE IMAGE
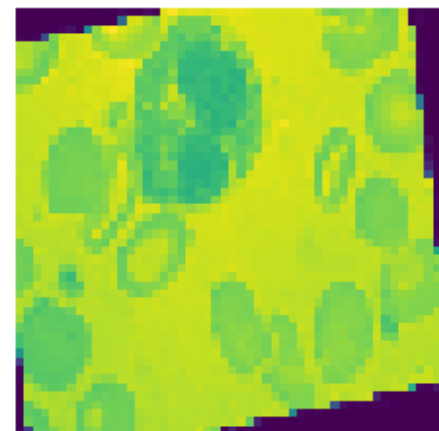

```
Resnet Deep Learning
------------------------------

1.Accuracy is : 98.61373901367188 %

2.Loss is    : 1.386260986328125


==========================================
---------------- Prediction ----------------
==========================================

----------------------

 Identified = EOSINOPHIL

----------------------
```

CONCLUSION

In this study, the deep learning is applied and analyse the blood cell images. The blood cell coloured and ground truth image data are taken as input data and applied into pre-processing method. In pre-processing method, the images are resized and converted into array. Then it processed into feature selection method, in this method the dataset is split into training dataset and testing dataset. After that all the images are resized and convert into array. Finally, the classification method is used to segment the blood cell by comparing coloured and ground truth images. Deep learning segmentation algorithm of CNN and RESNET is implemented and predict the result based on accuracy and error rate.

REFERENCES

[1] P. K. Das, S. Meher, R. Panda, and A. Abraham, "A review of automated methods for the detection of sickle cell disease," IEEE Rev. Biomed. Eng., vol. 13, pp. 309–324, Jan. 2020.

[2] P. K. Mishra, S. Agrawal, R. Panda, and A. Abraham, "A novel type-2 fuzzy C-means clustering for brain MR image segmentation," IEEE Trans. Cybernet., early access, Jun. 22, 2020, doi: 10.1109/TCYB.2020.2994235.

[3] C. Panagiotakis and A. A. Argyros, "Cell segmentation via region-based ellipse fitting," in Proc. 25th IEEE Int. Conf. Image Process. (ICIP), 2018, pp. 2426–2430, Doi: 10.1109/ICIP.2018.8451852.

[4] S. Zafari, T. Eerola, J. Sampo, H. Kalviainen, and H. Haario, "Segmentation of overlapping elliptical objects in silhouette images," IEEE Trans. Image Process., vol. 24, no. 12, pp. 5942–5952, Dec. 2015.

[5] D. K. Prasad, M. K. Leung, and C. Quek, "ElliFit: An unconstrained, non-iterative, least squares based geometric Ellipse Fitting method," Pattern Recognit., vol. 46, no. 5, pp. 1449–1465, 2013.

[6] C. Meng, Z. Li, X. Bai, and F. Zhou, "Arc adjacency matrix-based fast ellipse detection," IEEE Trans. Image Process., vol. 29, pp. 4406–4420, Feb. 2020.

[7] J. Li et al., "Automatic fetal head circumference measurement in ultrasound using random forest and fast ellipse fitting," IEEE J. Biomed. Health Inform., vol. 22, no. 1, pp. 215–223, Jan. 2018.

[8] M. González-Hidalgo, F. A. Guerrero-Peña, S. Herold-García, ˜ A. Jaume-i-Capó, and P. D. Marrero-Fernández, "Red blood cell cluster ´ separation from digital images for use in sickle cell disease," IEEE J. Biomed. Health Inform., vol. 19, no. 4, pp. 1514–1525, Jul. 2015.

[9] F. Azhar and T. Tjahjadi, "Significant body point labeling and tracking," IEEE Trans. Cybernet., vol. 44, no. 9, pp. 1673–1685, Sep. 2014.

[10] M. Winter, W. Mankowski, E. Wait, E. C. De La Hoz, A. Aguinaldo, and A. R. Cohen, "Separating touching cells using pixel replicated elliptical shape models," IEEE Trans. Med. Image., vol. 38, no. 4, pp. 883–893, Apr. 2019.

[11] S. Chen and J. Epps, "Efficient and robust pupil size and blink estimation from near-field video sequences for human–machine interaction," IEEE Trans. Cybernet., vol. 44, no. 12, pp. 2356–2367, Dec. 2014.

[12] B. Sheng et al., "Retinal vessel segmentation using minimum spanning superpixel tree detector," IEEE Trans. Cybernet., vol. 49, no. 7, pp. 2707–2719, Jul. 2019.

[13] Tareef et al., "Multi-pass fast watershed for accurate segmentation of overlapping cervical cells," IEEE Trans. Med. Image., vol. 37, no. 9, pp. 2044–2059, Sep. 2018.

[14] X. Bai, Y. Zhang, H. Liu, and Z. Chen, "Similarity measure-based possibilistic FCM with label information for brain MRI segmentation," IEEE Trans. Cybernet., vol. 49, no. 7, pp. 2618–2630, Jul. 2019.

[15] H. Xu, C. Lu, R. Berendt, N. Jha, and M. Mandal, "Automatic nuclear segmentation using multiscale radial line scanning with dynamic programming," IEEE Trans. Biomed. Eng., vol. 64, no. 10, pp. 2475–2485, Oct. 2017

[16] H. Zhao, J. Shi, X. Qi, X. Wang, and J. Jia, "Pyramid scene parsing network," in Proc. IEEE Conf. Compute. Vis. Pattern Recognition. (CVPR), Jul. 2017, pp. 2881–2890.

[17] O. Ronneberger, P. Fischer, and T. Brox, "U-Net: Convolutional networks for biomedical image SEG-mentation," in Proc. Int. Conf. Med. Image Compute. Compute. -Assist. Intervent., Cham, Switzerland: Springer, Nov. 2015, pp. 234–241.

[18] Z. Zhou, M. M. R. Siddiquee, N. Tajbakhsh, and J. Liang, "UNet++ A nested U-Net architecture for medical image segmentation," in Proc. Int. Workshop Deep Learn. Med. Image Anal., Cham, Switzerland: Springer, Sep. 2018, pp. 3–11.

[19] C. Stringer, T. Wang, M. Michaelos, and M. Pachitariu, "Cell pose: A generalist algorithm for cellular segmentation," Nature Methods, vol. 18, no. 1, pp. 100–106, Jan. 2021.

[20] U. Schmidt, M. Weigert, C. Broaddus, and G. Myers, "Cell detection with star-convex polygons," in Proc. Int. Conf. Med. Image Compute. Compute. - Assist. Intervent., Jun. 2018, pp. 265–273.

[21] S. Teng, J. Wu, Y. Chen, H. Fan, X. Cao, and Z. Li, "Semi-supervised leukocyte segmentation based on adversarial learning with reconstruction enhancement," IEEE Trans. Instrum. Meas., vol. 71, pp. 1–11, 2022.

[22] M. Sandler, A. Howard, M. Zhu, A. Zhmoginov, and L.-C. Chen, "MobileNetV2: Inverted residuals and linear bottlenecks," in Proc. IEEE/CVF Conf. Compute. Vis. Pattern Recognition., Jun. 2018, pp. 4510–4520.

[23] S. Yin, H. Deng, Z. Xu, Q. Zhu, and J. Cheng, "SD-UUNet: A novel segmentation framework for CT images of lung infections," Electronics, vol. 11, no. 1, p. 130, Jan. 2022.

[24] B. Li, S. Liu, F. Wu, G. Li, M. Zhong, and X. Guan, "RT-UUNet: An advanced network based on residual network and transformer for medical image segmentation," Int. J. Intel. Syst., vol. 37, no. 11, pp. 8565–8582, Aug. 2022.

[25] N. Akram, S. Adnan, M. Asif, S. M. A. Imran, M. N. Yasir, R. A. Naqvi, and D. Hussain, "Exploiting the multiscale information fusion capabilities for aiding the leukemia diagnosis through white blood cells segmentation," IEEE Access, vol. 10, pp. 48747–48760, 2022.

[26] S. Woo, J. Park, J. Y. Lee, and I. S. Kweon, "CBAM: Convolutional block attention module," in Proc. Eur. Conf. Compute. Vis. (ECCV), Sep. 2018, pp. 3–19.

[27] L. Liu, H. Jiang, P. He, W. Chen, X. Liu, J. Gao, and J. Han, "On the variance of the adaptive learning rate and beyond," 2019, arXiv:1908.03265.

[28] T. Tieleman and G. Hinton, "RMSProp: Divide the gradient by a running average of its recent magnitude," COURSERA Neural Networks Mach. Learn., vol. 4, no. 2, pp. 26–31, 2012.

[29] I. Tolstikhin, "MLP-mixer: An all-MLP architecture for vision," in Proc. 35th Conf. Neural Inf. Process. Syst., vol. 34, 2021, pp. 24261–24272.

[30] F. I. Diakogiannis, F. Waldner, P. Caccetta, and C. Wu, "ResUNet– A: A deep learning framework for semantic segmentation of remotely sensed data," ISPRS J. Photogramm. Remote Sens., vol. 162, pp. 94–114, Apr. 2020.